
Volume 61, issue 9, November 2009
ISSN 1359-6462
ELSEVIER
Scripta MATERIALIA
A LETTERS JOURNAL
STRUCTURE
PROPERTIES
THEORY
PROCESSING
FUNCTION
Available online at ScienceDirect www.sciencedirect.com
www.elsevier.com/locate/scriptamat

Available online at www.sciencedirect.com
ScienceDirect
Scripta Materialia 61 (2009) 887–890
Scripta MATERIALIA
www.elsevier.com/locate/scriptamat

Tensile and low-cycle fatigue properties of Mg–2.8% Al–1.1% Zn–0.4% Mn alloy along the transverse and rolling directions

F. Lv, F. Yang, Q.Q. Duan, T.J. Luo, Y.S. Yang, S.X. Li and Z.F. Zhang*

Shenyang National Laboratory for Materials Science, Institute of Metal Research, Chinese Academy of Sciences, 72 Wenhua Road, Shenyang 110016, China

Received 16 June 2009; revised 30 June 2009; accepted 21 July 2009
Available online 25 July 2009

The tensile, compressive and low-cycle fatigue properties of a rolled magnesium alloy Mg–2.8% Al–1.1% Zn–0.4% Mn (AZ31) along the transverse direction (TD) and rolling direction (RD) were investigated. The results show that both the strength and elongation of the TD samples are higher than those of the RD samples; consequently, the low-cycle fatigue properties of the TD samples are better than those of the RD samples in the total strain amplitude range from 0.2% to 0.6%, due to the effects of texture and microstructures.

Keywords: AZ31 Mg alloy; Rolling; Tension; Compression; Low-cycle fatigue

Magnesium alloy is a potential structural material that has a high strength-to-weight ratio, good machinability and recyclability [1]. These advantages make it very attractive for the automotive and aerospace industries [2,3]. As structural materials in service, magnesium alloys are usually subjected to repeated loading; therefore, the cyclic deformation behavior of these materials needs to be further investigated for safety reasons. There have been many studies on the fatigue properties of wrought magnesium alloys [4–8], but only a limited number have focused on rolled ones [5,9]. It is well known that a certain texture is easily formed in rolled magnesium alloys [10], leading to anisotropy of their mechanical properties; however, there are few reports which reveal the differences in the tensile, compressive and low-cycle fatigue properties of magnesium alloys along the transverse and rolling directions.

In wrought magnesium alloys, the texture has a significant effect on the plastic deformation behaviors, and the basal plane orientation influences the tensile and compressive strengths greatly; further, the texture plays an important role in the fatigue properties, as reported previously [6,11]. It has been recognized that better ductility is propitious for the improvement of low-cycle fatigue properties, while high strength is beneficial for the increase in high-cycle fatigue properties [12]. Therefore, the fatigue lifetime will be different in a rolled magnesium alloy when there is strength anisotropy along the transverse direction (TD) and rolling direction (RD). In this study, it was interesting to find that both the strength and the elongation of the TD samples are higher than those of the RD samples in a rolled AZ31 magnesium alloy sheet. Furthermore, the tensile, compressive and low-cycle fatigue properties along the TD and RD in the AZ31 alloy are compared.

Rolled AZ31 alloy sheet (Mg–2.8% Al–1.1% Zn–0.4% Mn, wt.%) was used in the present study. The materials were rolled for three passes to form a 4 mm thick sheet at 623, 573 and 298 K, respectively, then annealed at 623 K for 15 min. The specimens for tension and compression were cut along the RD and TD respectively. The gauge section of the tensile specimens was 25 mm and the dimensions of the compressive specimens were $4 \times 4 \times 8\ mm^3$. The tensile and compressive tests were conducted on an Instron-8801 testing machine at a constant strain rate of $1 \times 10^{-3}\ s^{-1}$. The low-cycle fatigue samples were also cut from the sheet along the RD and TD according to ASTM E606. Low-cycle fatigue tests were conducted on an Instron-8801 fatigue testing machine with a frequency of 0.5 Hz and a strain ratio of $S = -1$ in the total strain amplitude range from 0.2% to 0.6% at room temperature in air. The specimen at the total

* Corresponding author. Tel.: +86 24 23971043; e-mail: zhfzhang@imr.ac.cn

1359-6462/$ - see front matter © 2009 Acta Materialia Inc. Published by Elsevier Ltd. All rights reserved.
doi:10.1016/j.scriptamat.2009.07.023

strain amplitude of 0.2% was cyclically deformed through 50,000 cycles, then was subjected to a load-controlled test with a frequency of 30 Hz. The fracture morphologies were observed with a LEO-Supra35 scanning electron microscope.

Figure 1(a) and (b) show the texture and microstructure of the rolled AZ31 sheet respectively. There is a strong basal texture in the sheet, with a maximum intensity of 9.29. Figure 1(b) shows the optical microstructure of the sample observed on the three planes; it can be seen that most grains on the ND plane are equiaxed, with an average size of about 10 μm.

Figure 2(a) shows the engineering stress–strain curves of the materials along the TD and RD under tensile and compressive loadings. The ultimate tensile strengths of the TD and RD samples are 306 and 280 MPa, respectively. The elongation of the TD sample is nearly 25%, prominently higher than that (~13%) of the RD sample. This indicates that both the tensile strength and the elongation of the AZ31 alloy display simultaneous increasing trends from the RD to the TD, which was not observed previously in rolled AZ alloys [13,14]. In addition, the compressive yield strength of the RD and TD samples are found to be much lower than their tensile yield strengths; however, their compressive fracture strengths are significantly higher than the tensile ones, which can be attributed to the easier twinning under compression [11]. The tension/compression asymmetry of extruded AZ magnesium alloys was also reported by Bohlen et al. [15], who discussed the grain size and solute content effects. Meanwhile, the maximum compressive strength and maximum plastic strain of the TD sample are also higher than those of the RD sample, showing a similar trend to their tensile properties. The great differences in the compressive and tensile properties must significantly influence their fatigue damage processes and fatigue lifetime; this will be discussed later.

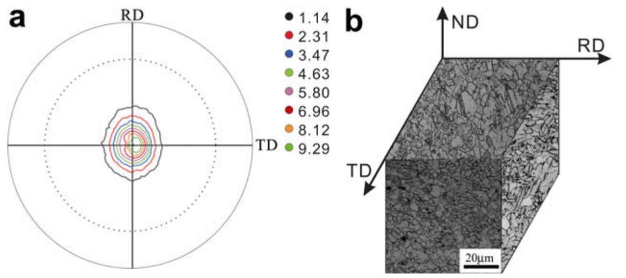

Figure 1. (a) {0 0 0 2} pole figure for rolled AZ31 alloy; (b) optical images of the microstructures observed in three planes.

Dobron et al. [16] and Balic et al. [17] reported the tensile strength of rolled AZ31 alloy with the same trend, i.e. the strength of the TD sample is definitely higher than that of the RD sample. However, the elongation of the TD sample was not greater than that of the RD sample, as indicted in Table 1. In addition, Balic et al. [17] and Agnew et al. [18] performed tensile tests on a rolled AZ31-H24 sheet at room and elevated temperatures. They found that the strength of the TD samples was higher than that of the RD samples while the difference in the elongation was not so obvious. A similar result was also reported by Koike and Ohyama [14] in a rolled AZ61 magnesium alloy, though with the difference that the strength and elongation did not increase synchronously. Yi et al. [19] also explained the difference in the strength of the extruded AZ31 with texture evolution. The detailed mechanism will be discussed elsewhere.

Since the tensile and compressive strengths, elongation and compressive plasticity of the TD samples were

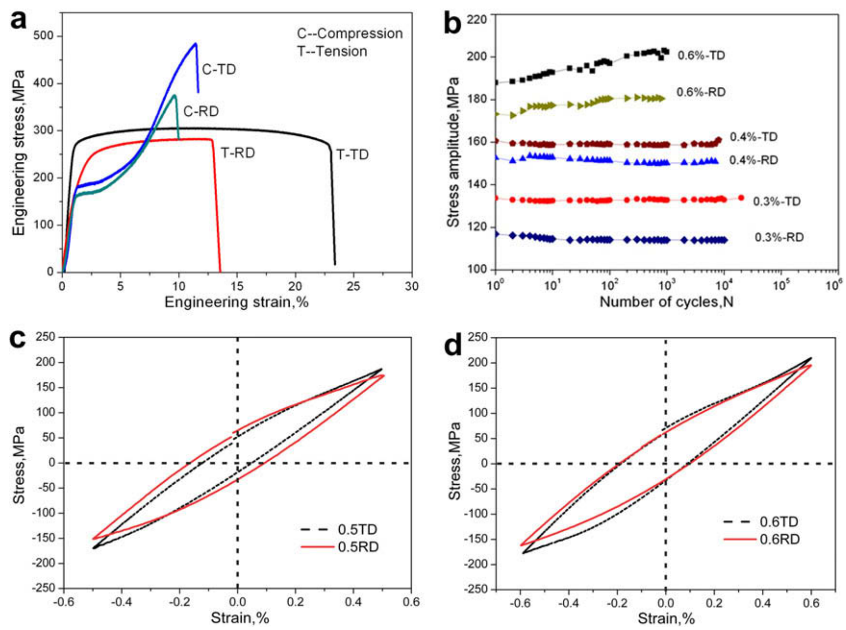

Figure 2. (a) The tensile and compressive stress–strain curves of the samples in the TD and RD at a strain rate of 5×10^{-3} s^{-1}; (b) cyclic stress responses of the TD and RD samples at total strain amplitudes of 0.3, 0.4 and 0.6%; (c and d) hysteresis loops of the RD and TD samples at total strain amplitudes of 0.5% and 0.6%, respectively, at the first and after several circles.

Table 1. Mechanical properties of the current magnesium alloy sheet and other magnesium alloys with similar compositions [15,16].

Compositions	Heat treatment	Direction	TYS (MPa)	UTS (MPa)	El (%)
Mg–2.8% Al–1.1% Zn–0.4% Mn	O-temper	RD	195	280	13
		TD	260	306	24
Mg–3% Al–1% Zn [15]	H24	RD	220	280	21
		TD	265	295	17
Mg–3% Al–0.9% Zn–0.15Mn [16]	H24	RD	190	340	15
		TD	220	380	15

TYS, tensile yield strength; UTS, ultimate tensile strength; EL, elongation.

always higher than those of the RD sample, it was necessary to reveal whether the fatigue properties of the samples displayed a similar trend. Figure 2(b) shows the cyclic stress responses of the TD and RD samples with increasing cyclic number. It can be seen that under the same total strain amplitude, the cyclic stresses of the TD samples are always higher than those of the RD samples. This can be explained by both the tensile and compressive strengths of the TD samples being higher than those of the RD samples. Apparently, there was no obvious cyclic hardening or softening behavior under the low total strain amplitudes of 0.3% or 0.4%, while a slight cyclic hardening occurred at a total strain amplitude of 0.6% for both the TD and RD samples. Figure 2(c) and (d) demonstrate the hysteresis loops at different total strain amplitudes, of 0.5% and 0.6% respectively. The shape of the loops is rather symmetrical and is far different from those observed by Yin et al. [8] for extruded AZ31 alloy. The formation of the symmetrical loops in the current samples may be caused by the grain size and texture. The extruded AZ31 observed by Yin et al. [8] had a fibrous texture and a larger grain size; therefore deformation twins were easy to form during compression, while the tension–compression asymmetry phenomenon is serious and induces the sigmoid hysteresis loop. However, in the present study, different basal texture and smaller grain size make the shape of the hysteresis loop not so asymmetric.

The difference in the tensile and compressive properties should have a definite effect on the samples' fatigue properties. Figure 3(a) shows the curves of total strain amplitude vs. number of cycles to failure. It is apparent that the low-cycle fatigue lifetime of the TD samples is higher than that of the RD samples under the strain-controlled tests. This indicates that the higher elongation and compressive plasticity of the TD samples improve their low-cycle fatigue life compared with that of the RD samples. As shown in Figure 2(b), the cyclic stresses of the TD samples are always higher than those of the RD samples under the same total strain amplitudes. We selected the stress amplitudes at the half of lifetime as the applied stress amplitudes, and the *S–N* curves of the TD and RD samples are shown in Figure 3(b). It can be seen that under the same stress amplitude the fatigue life of the TD samples is also higher than that of the RD samples. According to the above results, one can predict that the fatigue life of the TD samples will be longer than that of the RD samples under stress-controlled conditions. This will be systematically summarized in a coming paper.

As can be seen in Figure 1(a), the basal texture could explain the mechanical anisotropy, the ellipse-shaped intensity contour indicating that grains tend to be oriented with their basal planes inclined more towards RD than TD. Also, the Schmid factor for basal <*a*> slip within the grains in the RD samples is larger than that for the TD samples. Other slip systems (especially prismatic slip [14]) could also contribute to the higher strength and elongation of the TD samples. Dobron et al. [16] and Balic et al. [17] also attributed the higher strength of TD samples to the dislocation on the basal and non-basal planes, as well as deformation twinning. The macroscopic fracture morphologies of the TD and RD samples are shown in Figure 4. It can be seen that necking occurred in the TD sample and the microscopic fracture indicates better ductility with large and deep dimples (see Figure 4(b) and (d)). On the other hand, the failure features of the RD sample are macroscopic shear fracture with shallower shear dimples on the microscale, as shown in Figure 4(a) and (c). The above

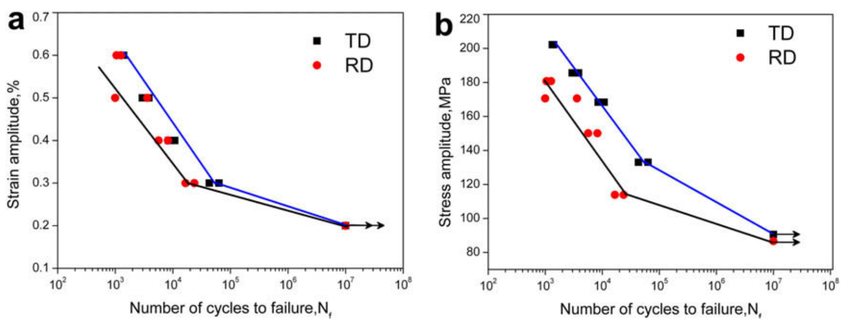

Figure 3. (a) Total strain amplitude as a function of the number of cycles to failure for the RD and TD samples; (b) stress amplitude vs. number of cycles to failure curves for the RD and TD samples.

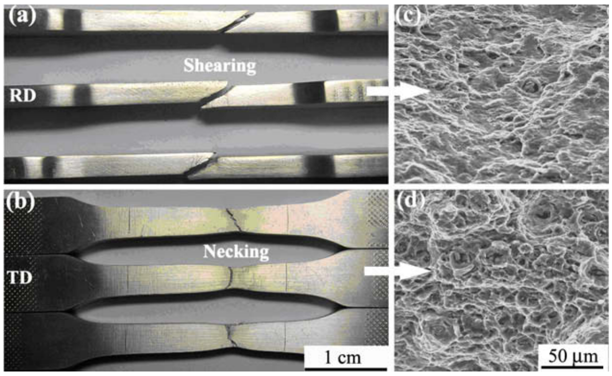

Figure 4. Macroscopic and microscopic tensile fracture features of the RD and TD samples.

fracture features provide some indirect evidence for the differences in slip deformation between the TD and RD samples.

Ishihara et al. [5] reported that, in extruded AZ31 alloy, the tensile strength of the parallel extrusion (EP) samples was higher than that of the vertical extrusion (EV) samples, so the corresponding fatigue-life of the EP samples was longer than that of the EV samples under stress-controlled conditions. Zuberova et al. [7] compared the fatigue performances of AZ31 alloy processed by three routes, and found that the hot-rolled AZ31 alloy had the highest fatigue limit under stress-controlled tests because the strength was the highest under such processing conditions. Therefore, when the TD samples have higher elongation and strength than the RD samples, this endows them with better fatigue properties, as shown in Figure 3(a) and (b). This finding suggests that the mechanical properties of AZ31 magnesium alloy can be optimized even further for structural applications by producing higher strength, higher elongation and better fatigue properties through suitable rolling processes.

In summary, the current results provide new evidence that the mechanical properties of AZ31 magnesium alloy can be optimized to have higher strength, higher elongation and better fatigue properties through suitable rolling processes. It has been confirmed that, for the same material, the higher elongation corresponds to a longer strain-controlled fatigue life and the higher tensile strength yields a longer stress-controlled fatigue life. This finding should be helpful in achieving the optimum design of rolled AZ31 magnesium alloy for potential applications.

The authors thank Ms. W. Gao, Mr. H.H. Su, Prof. H. Mughrabi, Prof. G.Y. Li and Prof. D.L. Chen. This work was financially supported by the National Natural Science Foundation of China (NSFC) under Grant Nos. 50625103 and 50890173 and the National Basic Research Program of China under Grant No. 2007CB613705.

[1] B.L. Mordike, T. Ebert, Mater. Sci. Eng. A 303 (2001) 37.
[2] A.A. Luo, JOM 54 (2002) 42.
[3] S.R. Agnew, JOM 56 (2004) 1543.
[4] F. Yang, S.M. Yin, S.X. Li, Z.F. Zhang, Mater. Sci. Eng. A 491 (2008) 131.
[5] S. Ishihara, Z.Y. Nan, T. Goshima, Mater. Sci. Eng. A 468 (2007) 214.
[6] Z.B. Sajuri, Y. Miyashita, Y. Hosokai, Y. Mutoh, Int. J. Mech. Sci. 48 (2006) 198.
[7] Z. Zuberova, L. Kunz, T.T. Lamark, Y. Estrin, M. Janecek, Metall. Mater. Trans. A 38 (2007) 1934.
[8] S.M. Yin, H.J. Yang, S.X. Li, S.D. Wu, F. Yang, Scripta Mater. 58 (2008) 751.
[9] S. Hasegawa, Y. Tshuchida, H. Yano, M. Matsui, Int. J. Fatigue 29 (2007) 1839.
[10] A. Styczynski, Ch. Hartig, J. Bohlen, D. Letzig, Scripta Mater. 50 (2004) 943.
[11] L. Wu, A. Jain, D.W. Brown, G.M. Stoica, S.R. Agnew, B. Clausen, D.E. Fielden, P.K. Liaw, Acta Mater. 56 (2008) 688.
[12] S. Suresh, Fatigue of Materials, Cambridge University Press, Cambridge, 1998.
[13] A. Jager, P. Lukac, V. Gartnerova, J. Bohlen, K.U. Kainer, J. Alloys Compd. 378 (2004) 184.
[14] J. Koike, R. Ohyama, Acta Mater. 53 (2005) 1963.
[15] J. Bohlen, P. Dobron, J. Swiostek, D. Letzig, F. Chmelik, P. Lukac, K.U. Kainer, Mater. Sci. Eng. A 462 (2007) 302.
[16] P. Dobron, J. Bohlen, F. Chmelik, P. Lukac, D. Letzig, K.U. Kainer, Kovov Mater. 45 (2007) 129.
[17] J. Balic, P. Lukac, J. Bohlen, K.U. Kainer, Kovov Mater. 45 (2007) 135.
[18] S.R. Agnew, O. Duygulu, Int. J. Plast. 21 (2005) 1161.
[19] S.B. Yi, C.H.J. Davies, H.G. Brokmeier, R.E. Bolmaro, K.U. Kainer, J. Homeyer, Acta Mater. 54 (2006) 549.